DOI: 10.12923/cipms-2025-0042 Curr. Issues Pharm. Med. Sci., Vol. 38, No.4, Pages 264-269

Current Issues in Pharmacy and Medical Sciences
Formerly ANNALES UNIVERSITATIS MARIAE CURIE-SKLODOWSKA, SECTIO DDD, PHARMACIA

journal homepage: https://czasopisma.umlub.pl/curipms

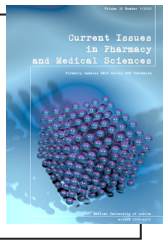

Synthesis, characterization, and antibacterial properties of selected glucose derivatives

Hawraa Mohammed Sadiq*

Department of Chemistry, College of Science, University of Kufa, Najaf, Iraq

ARTICLE INFO

Received 30 June 2024
Accepted 28 April 2025

Keywords:
carbohydrates,
protection,
Escherichia coli,
Staphylococcus aureus,
azide.

ABSTRACT

A multistep synthetic route was developed for the preparation of a diazido compound starting from methyl α-D-glucopyranoside **1**. The synthesis began with protection of the C-4 and C-6 hydroxyl groups using a benzylidene protecting group. Compound **2** was subsequently reacted under phase-transfer conditions with bis (2-chloroethyl) ether to afford the bis-chloro derivative **3**. Compound **3** was then converted into a more effective leaving-group derivative, namely the iodide compound **4**. Finally, nucleophilic substitution of the iodide groups with azide ions was carried out by reacting compound **4** with sodium azide in dimethylformamide, yielding the target diazido derivative **5**.
In addition, the synthesized compounds were evaluated for antibacterial activity against *Escherichia coli* and *Staphylococcus aureus* using the agar well diffusion method. The results demonstrated moderate antibacterial activity against both tested strains. Structural characterization of all synthesized compounds was performed using infrared (IR) spectroscopy and nuclear magnetic resonance spectroscopy (^{1}H NMR and ^{13}C NMR).

INTRODUCTION

Carbohydrates are highly functionalized compounds with well-defined stereochemistry due to the presence of chiral centers with hydroxyl (-OH) groups directed to specific positions. These hydroxyls exhibit various reactivities, which opens the path for the synthesis of a variety of derivatives [1]. Carbohydrates possess diverse biological roles in almost all living organisms [2].

The driving forces of their activities are attributed to their chiral centers [3], their conjugation with other biomolecules, and their specific positions within cells. Based on auxiliary mediation strategies [4], varying functionalized stereogenic centers are present in carbohydrate moieties, making them suitable compound templates for investigating important rigid architectures involving known stereochemistry [5,6].

Multi-step synthesis, designed by many organic chemists, often requires a series of protection steps to ensure one functional group remains inert to a particular reagent [7]. Protecting groups are essential for chemo- and regioselective manipulation in synthesis. Although a wide range of protecting groups is available to carbohydrate chemists, their stability and orthogonality make the selection difficult [8].

Carbohydrates not only play crucial roles as energy storage or as sources of biomaterials but also have significant roles in diverse biological recognition and regulation processes such as microbial infections and immune responses [9]. The pyranoside sugars are often utilized in structure-activity relationship studies of drugs [10]. The differentiation of hydroxyl groups in carbohydrates remains a long-standing challenge [11]. Although enzymatic methodologies are typically effective for the efficient functionalization of hydroxyl groups in carbohydrates, it remains complicated to selectively discriminate between the hydroxyl groups of sugars using non-enzymatic approaches [12].

Bacteria live in various environments and are continually exposed to diverse stimuli, as surrounding chemical compounds and physical conditions change [13].

Escherichia coli is a type of bacteria found in the human intestines that plays an important role in digestion. These bacteria have diagnostic value when infection occurs, as urinary tests are performed in 80% of cases [14]. *Staphylococcus aureus* is ubiquitous in nature. It is a major human pathogen that can grow in inappropriately stored food [15], causing a diversity of diseases in humans such as abscesses, pneumonia, meningitis, and mastitis [16].

MATERIALS AND INSTRUMENTS

Experimental section

All chemicals and solvents were purchased and used without further purification. α-methyl-D-glucose,

* **Corresponding author**
e-mail: hawraam.hmeidi@uokufa.edu.iq

α,α-dimethoxytoluene, anhydrous sodium sulfate, sulfonic acid monohydrate, bis- (2-chloroethyl) ether, sodium bicarbonate, sodium hydroxide (NaOH), tetrabutylammonium bromide, sodium iodide (Na_2I), sodium azide (NaN_3), acetone, chloroform, ethanol, ethyl acetate, n-hexane, and toluene were obtained from Sigma Aldrich as analytical grades. ^1H and ^{13}C NMR spectra were recorded on a Bruker advance NEO at 400 MHz and 101 MHz, respectively, using $CDC1_3$, FT-IR spectra were recorded using an Alpha-Bruker (Germany).

Synthesis

***Methyl-4,6-O-benzylidene-α-D-glucopyranoside* 2**

Methyl-α-D-glucopyranoside **1** (12 g, 61.85 mmol) and α,α-dimethoxytoluene (12 mL,78.24 mmol) were dissolved in DMF (100 mL) and a catalytic amount of sulfonic acid monohydrate was added. The mixture was heated at 75°C in a rotary evaporator under vacuum. The reaction progress was monitored by TLC (ethyl acetate: n-hexane, 1:1). Upon completion of the reaction, the solvent was evaporated, and the residue was dissolved in CHCl3 (30 mL), and washed with a saturated sodium bicarbonate solution (2×30 mL), followed by distilled water. The solvent was removed under vacuum, dried over Na_2SO_4, filtered, and the organic phase evaporated to furnish compound **2** (12.24 g, yield 88%) as a white fine powder [17].

***Methyl-4,6-O-benzylidene-2,3-bis[(2-chloroethoxy) ethyl]-α-D-glucopyranoside* 3**

A mixture of compound **2** (15 g, 53.19 mmol) and tetrabutylammonium bromide (12 g, 35.8 mmol) in bis- (2-chloroethyl) ether (150 mL), which served as both reactant and solvent, was mechanically stirred with the phase transfer catalyst (PTC) and a 50% NaOH solution (90 mL) at room temperature for 72 hours. The mixture was washed extensively with water. The excess bis (2-chloroethyl) ether was evaporated with the assistance of a co-solvent to prevent product decomposition, as a high temperature is required. Water was selected as the co-solvent, and the product was extracted into ethyl acetate. The combined organic phases were washed with water, dried over Na_2SO_4, filtered, and the solvent evaporated to furnish the product as a yellow syrup in almost quantitative yield (22.1 g, 78.36%) [18].

FT-IR data (cm^{-1}): 3459.5, 3351.5 (OH groups). 3061.8,3034.9 (H-aromatic), 2911.5, 2867.0 (H-aliphatic), 2000.0-1600,0 (overtone bands),1454.2, 1371.6 (C=C aromatic), 1298.2 (CH_2-Cl).

^1H-NMR (400 MHz, CDCl3) δ 3.14-3.26 (m, 1H), 3.26-3.37 (m, 1H), 3.33-3.41 (m, 1H), 3.37-3.47 (m, 1H), 3.43-3.57 (m, 4H), 3.53-3.67 (m, 8H), 3.63-3.75 (m, 4H), 3.81-4.00 (m, 5H), 4.26 (dd, J = 10.5, 5.0 Hz, 1H), 4.41 (d, J = 7.7 Hz, 1H), 5.46 (s, 1H), 7.30 (tdd, J = 4.7, 3.5, 1.5 Hz, 3H), 7.36-7.44 (m, 2H).

^{13}C-NMR (101 MHz, CDCl3) δ 42.63, 42.78, 42.81, 50.95, 66.11, 68.67, 70.80, 70.82,71.09, 71.15, 71.35, 72.39, 72.45, 80.76, 81.62, 82.68, 101.30, 103.79, 126.07, 128.26,129.05, 137.24.

***Methyl-4,6-O-benzylidene-2,3-bis[(2-iodo ethoxy)ethyl]-α-D-glucopyranoside* 4**

Compound **3** (30 g, 58.59 mmol) was dissolved in dry acetone (170 mL). NaI (36 g, 256.85 mmol) was added, and the solution was stirred under reflux for 24 h (monitored by TLC (ethyl acetate: n-hexane, 1:1)). When the starting material was consumed, the solvent was evaporated. The residue was dissolved in ethyl acetate (40 mL) and then washed with water (3×40 mL). The organic phase was dried over sodium sulfate, filtered, and then evaporated *in vacuo* to give compound **4** as a pale brown syrup (31 g, 76.73%) [19].

FT-IR data (cm^{-1}): 3063, 3036 (H-aromatic), 2911.6, 2865.1 (H-aliphatic), 1453 (C=C aromatic), 1185.4 (CH2-I).

^1H-NMR (400 MHz, $CDCl_3$) δ 7.28-7.42 (m, 5H, Ph), 5.45 (d, J = 0.9Hz, 1H, PhCH benzylidene), 4.41 (m, 1H, H-1), 4.39 (dd, J = 11.4, 1.6 Hz, 1H, H-6), 4.27 (m, 1H, H-3), 4.26 (m, 1H, H-4), 4.23 (dd, J= 11.5, 4.4 Hz, 1H, H-6), 3.85-3.96 (m, 17H, H-2, 6 OCH_2, 2 CH_2I), 3.62-3.66 (m, 1H ,H-5), 3.42-3.55 (d, J = 1.5 Hz, 3H, OCH_3).

^{13}C-NMR (125 MHz, CDCl3) δ 137.23, 126.03, 128.26, 129.06 (Ph), 103.78 (Ph-CH benzylidene), 101.30 (C-1), 82.68-80.75 (C-4, C-3, C-2), 72.45-66.11 (6 CH_2O ,C-5, C-6), 50.95 (CH_3), 4.85, 4.82 ($2CH_2$-I).

***Methyl-4,6-O-benzylidene-2,3-bis[(2-azidoethoxy) ethyl]-α-D-glucopyranoside* 5**

Compound **4** (6.78 g, 10 mmol) was mixed with sodium azide (1.0 g, 15 mmol) and dissolved in DMF (20 mL), then heated to 110°C for 48 hours. TLC showed the completion of the reaction. The DMF was evaporated *in vacuo*, and the product was extracted using an ethyl acetate/water mixture. The organic layer was separated, dried with sodium sulfate, filtered, and the solvent was evaporated to give compound **5**, which was further purified by column chromatography to yield (6.3 g, 85%) [20].

FT-IR data (cm^{-1}): 3063, 3036 (H-aromatic), 2911.6, 2865.1 (H-aliphatic), 1453 (C=C aromatic), 2097.08 (CH_2-N_3).

^1H-NMR (400 MHz, $CDCl_3$) δ 7.41-7.28 (m, 5H, Ph), 5.46 (s, 1H, PhCH benzylidene), .4.80 (d, $^3J_{1,2}$ = 3.7 Hz, 1H, H-1) 4.38-4.36 (m, 1H, H-2), 4.09-3.61 (m, 22H, H-3, H-4, H-5, H-6ax, H-6eq, 6 CH_2O, OCH_3), 2.81 (m, 4H, 2 CH_2-N_3).

^{13}C-NMR (100 MHz, $CDCl_3$) δ 137.42, 126.03, 128.26, 129.06 (Ph), 101.27 (PhCH benzylidene), 99.50 (C-1), 82.68, 82.28, 80.67 (C-4, C-3, C-2), 72.69, 71.10, 70.31, 69.69, 69.35, 69.30, 69.12, 69.06, (6 CH_2O) 62.39, 62.19 (C-5, C-6), 55.23 (OCH_3), 48.38, 48.18 ($2CH_2$-N_3).

Antibacterial activity

The agar well diffusion method [21] was used against two types of bacteria (*E. coli* and *S. aureus*). The two sugar derivatives **3** and **4** were studied [22]. Five clear isolated colonies of fresh culture were cultured in five milliliters and incubated at 37°C for 4-8 h. The resulting turbidity was calibrated. A sterile cotton swab was dipped into the suspension.

The swab was used to streak the entire surface of a Mueller-Hinton agar plate. Then, using a sterile cork borer, wells (7 mm diameter) were produced and filled with the two

derivative compounds, A_1 and A_2, at concentrations of 125, 250, 500, and 1000 µg/mL. The fifth well was filled with Penicillin G (1 µg/mL) as a control for both Gram-negative and Gram-positive bacteria. The Petri dishes were then incubated at 37°C for 24 h. The diameter of the growth inhibition zones, measured in millimeters, was used to determine the antibacterial activity [23,24].

RESULTS AND DISCUSSION

Synthesis of carbohydrate derivatives

The synthesis of bioactive compounds derived from methyl-α-D-glucose began with the treatment of α-methyl glucose **1** with α,α-dimethoxytoluene, catalyzed by TsOH·H2O in DMF, to yield 4,6-O-benzylidene-α-methyl-D-glucose **2** in good yield (Scheme 1).

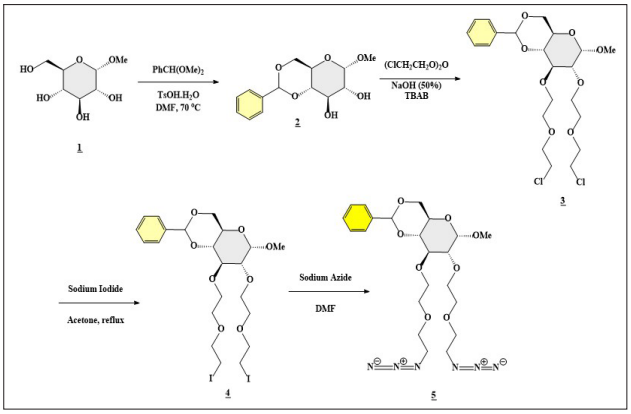

Scheme 1. Synthesis carbohydrate derivatives (2-5)

The second step involved a Williamson etherification reaction between the free hydroxyl groups at the carbons 2- and 3- positions of compound **2** with bis- (2-chloroethyl) ether in a basic medium, dissolved in DMF in the presence of phase transfer catalysts.

The FT-IR spectrum of compound **3** (Fig. 1) showed the disappearance of stretching vibrations in the 3450-3350 cm^{-1} range, corresponding to the absorption of OH-groups at C-2 and C-3. Furthermore, the signal appearing at 747 cm^{-1} can be attributed to the stretching vibrations of the CH_2-Cl bond.

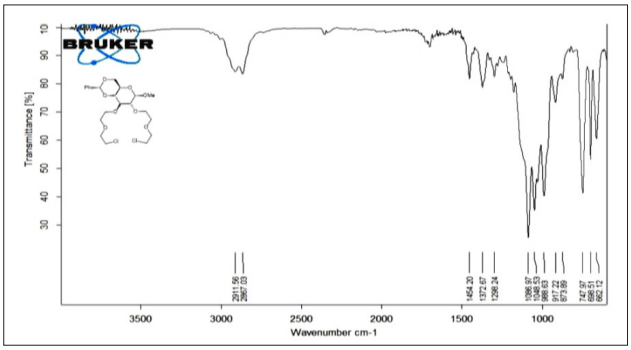

Figure 1. FT-IR spectrum of compound **3**

The ^{1}H-NMR data of compound **3** (Fig. 2) showed several multiplets in the 3-4 ppm range, which originate from the protons of the Cl-CH_2CH_2-CH_2CH_2 groups at the 3- and 4- carbon atoms of the glucopyranoside ring. Similarly, the ^{13}C-NMR spectrum of compound 3 (Fig. 3) showed carbon peaks in the 75-69 ppm region, which reflect the carbon numbers in the compound and are attributed to the carbons of both Cl-CH_2CH_2-CH_2CH_2 groups.

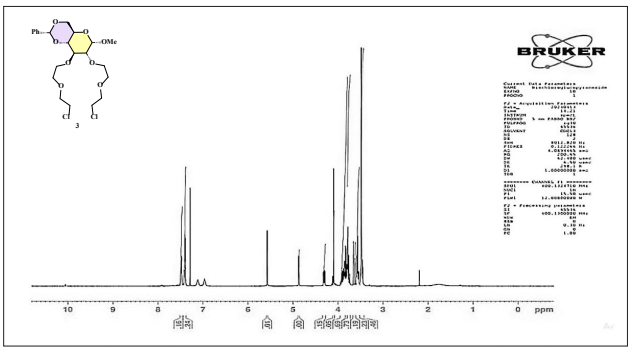

Figure 2. ^{1}H- NMR spectrum of compound **3**

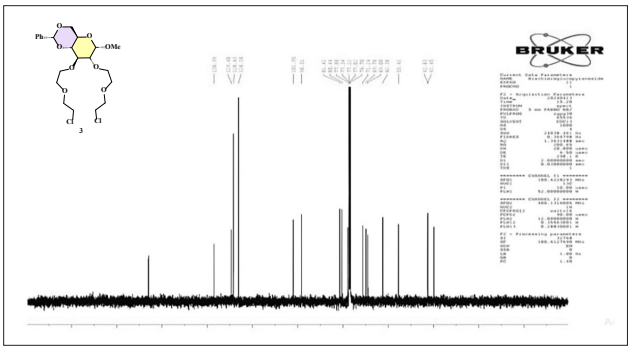

Figure 3. ^{13}C-NMR spectrum of compound **3**

In the third step, the carbon atoms in compound 3 are directly attached to the iodide. The reaction replaces the chlorine atoms with more reactive iodide atoms under easy reaction conditions using acetone and NaI. The sodium iodide dissolves when heated, and sodium chloride is created during the ripening of the reaction. The reaction was monitored by TLC, which indicated that the product was produced. No further purification was done, and compound **4** was used in the next step because the reaction did not produce anything.

The FT-IR spectrum of compound **4** (Fig. 4) showed the characteristic absorption bands of the product, the band at 617 cm^{-1} can be attributed to the stretching vibrations of the C-I bond.

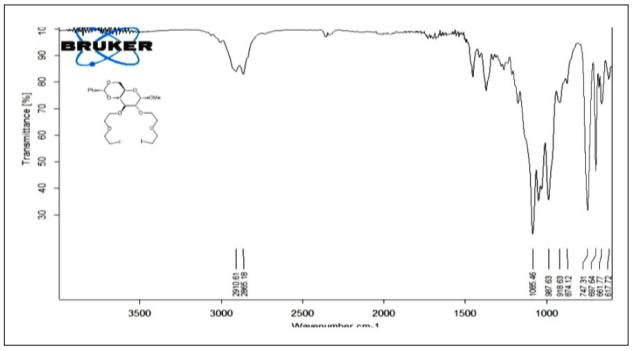

Figure 4. FT-IR spectrum of compound **4**

The ^{1}H-NMR data of compound **4** showed signals in the 3.80-3.63 ppm range for (OCH_2,CH_2I), 5.45 ppm (s, 1H) for the benzylidene proton, and signals in the 7.42-7.32 ppm range for the H-aromatic of the benzylidene group (Fig. 5).

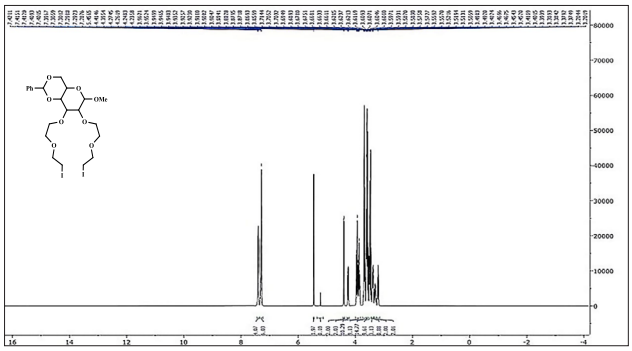

Figure 5. 1H-NMR spectrum of compound **4**

The ^{13}C-NMR spectrum of compound **4** showed new carbon signals in the 72.44−66.11 ppm range for (CH_2O), 4.84 & 4.81 ppm for (2 CH_2-I), 103.7 ppm for the benzylidene carbon, and 137.2,129.02,128.2,126 ppm for the C-aromatic of the benzylidene group (Fig. 6).

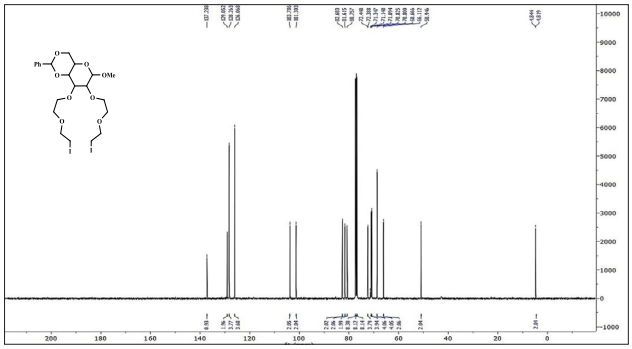

Figure 6. ^{13}C-NMR spectrum of compound **4**

Compound **4** was reacted with sodium azide in the next step to replace the iodine with azide groups, yielding the diazide **5**. The reaction of sodium azide with compound **4** was achieved in DMF solvent at a slightly elevated temperature. Compound **5** was characterized by FT-IR (Fig. 7), which indicated a strong azide band appearing in the 2100 cm^{-1} range. Additionally, the absence of the carbon-iodine band at 660 cm^{-1} confirmed the substitution. The reaction followed an S_N2 mechanism due to the good leaving group capability of iodine and the strong nucleophilicity of the azide group.

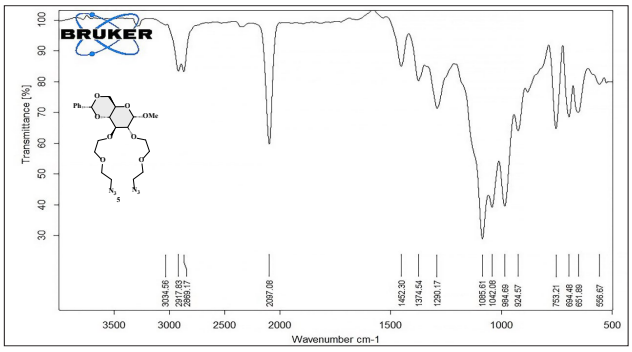

Figure 7. FT-IR spectrum of compound **5**

The ^{1}H-NMR spectrum (Fig. 8) showed characteristic peaks that changed due to the attachment of azide groups. Other peaks in the 4-3 ppm range showed some differences in shape, but there was no significant change in the proton spectrum due to the similar chemical shift observed for protons adjacent to either iodide or azide.

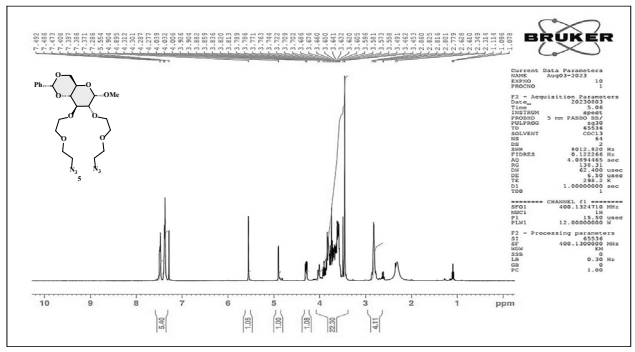

Figure 8. ^{1}H-NMR spectrum of compound **5**

The ^{13}C-NMR spectrum of compound **5** (Fig. 9) represented the characteristic carbon peaks. The carbons attached to iodine normally appear near 1-10 ppm on the spectrum, but these are absent in the azide derivative **5**. The new carbons in the 48.10 and 48.33 ppm region are attributed to the carbons directly attached to the azide. The other peaks for all carbons in the structure were found.

The assignment of all carbons and protons was confirmed by the 2-D NMR HSQC spectrum (Fig. 10), which indicates which carbon is directly attached to which proton in the molecules.

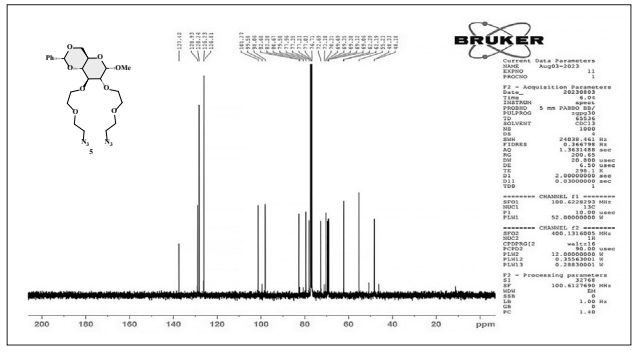

Figure 9. ^{13}C-NMR spectrum of compound

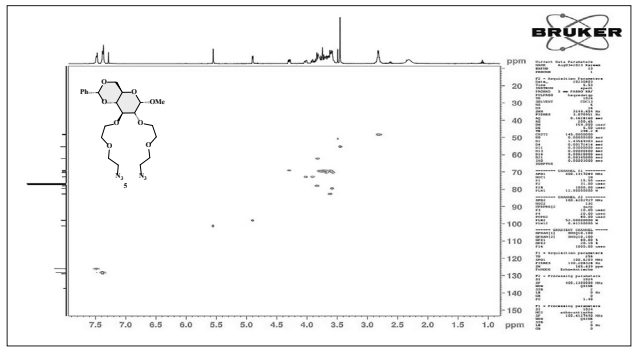

Figure 10. HSQCeditedGP spectrum of compound **5**

ANTIBACTERIAL ACTIVITY

Attributed to the chemical structure of both the bacteria and the sugar derivatives, interactions may occur either through the protein units of the cell membranes or by Van der Waals forces and H-bonding. *S. aureus* and *E. coli* were chosen due to their significance in the field of medicine,

as they are associated with numerous diseases, making the synthesis of compounds that can inhibit or kill these bacteria important. Table 1 shows that derivatives A_1 **3** and A_2 **4** exhibit a broad-spectrum efficiency in inhibiting the growth of both Gram-positive and Gram-negative bacteria when combined with standard antibiotics. The inhibition zone diameter increased with the concentration of these compounds. *E. coli* and *S. aureus* were selected for the antibacterial study due to their widespread presence in all environments. They are major causes of many diseases harmful to humans. To overcome bacterial resistance to antibiotics, sugar derivatives are compatible with bacterial components such as carbohydrates or glycolipids in the cell membrane, which increases the potential for interactions leading to biologically active sugar derivatives. Table 1 shows that derivatives A_1 and A_2 have a high ability to inhibit the growth of both *E. coli* and *S. aureus*. The inhibition zones increase as the concentration of these derivatives increases.

Table 1. Inhibition of bacterial growth (inhibition diameter) by A_1 **3** and A_2 **4** (mm)

Material	Concentration (µg/ml)	*S. aureus*	*E. coli*
3	125	0	0
3	250	0	0
3	500	11	12
3	1000	17	18
Penicillin G	1000	16	14
4	125	0	0
4	250	0	0
4	500	13	11
4	1000	20	17
Penicillin G	1000	15	13

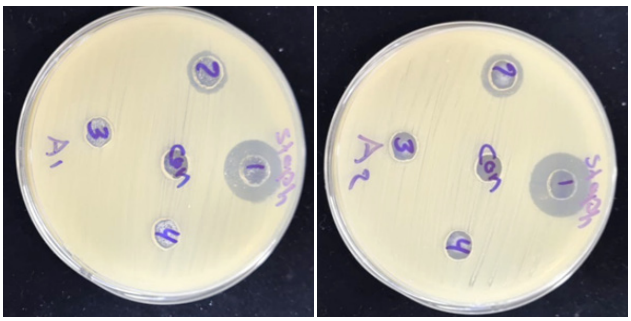

Figure 11. Inhibition zones of (A_1 **3** and A_2 **4**) to bacteria (S. *aureus*)

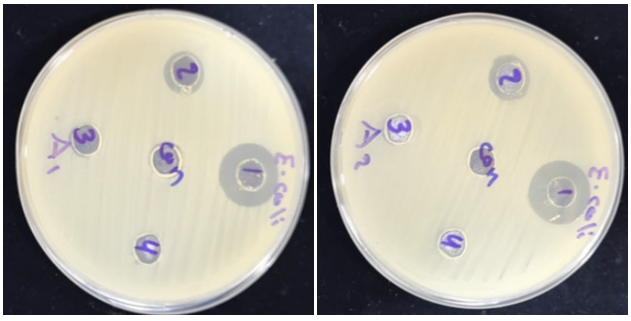

Figure 12. Inhibition zones of (A_1 **3** and A_2 **4**) to bacteria (*E. coli*)

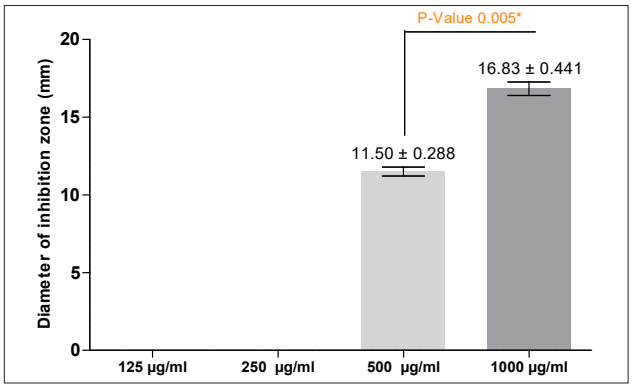

Figure 13. Effect of A1 compound against *Staphylococcus aureus* growth

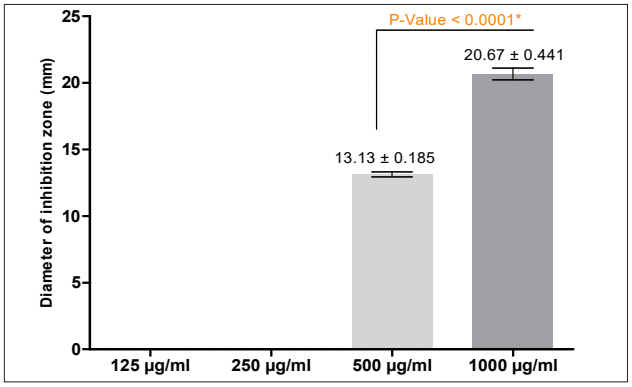

Figure 14. Effect of A2 compound against *Staphylococcus aureus* growth

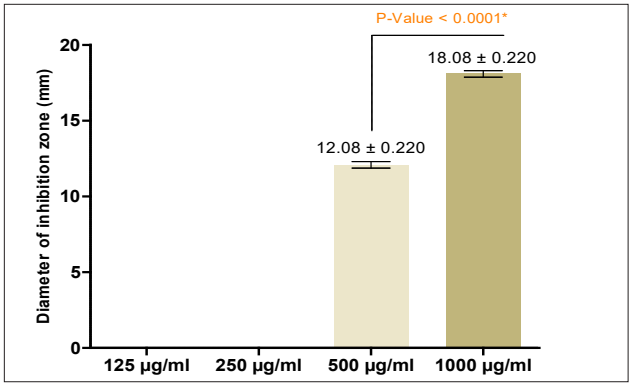

Figure 15. Effect of A1 compound against *Escherichia coli* growth

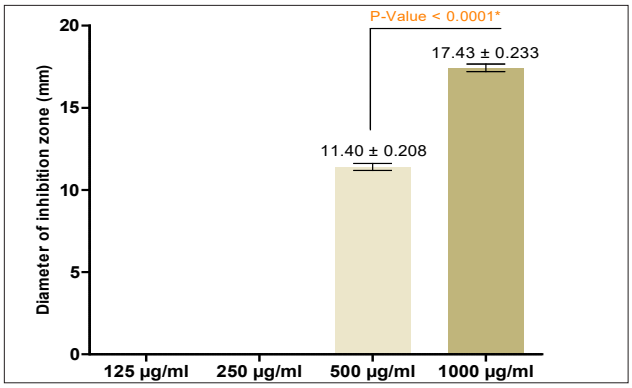

Figure 16. Effect of A2 compound against *Escherichia coli* growth

CONCLUSION

In conclusion, the synthesis of glucose derivatives with two halogen atoms was successfully achieved with high yields. The straightforward use of protecting groups allowed for the synthesis at specific positions, namely **2** and **3** on the pyranoside ring. The chloro-derivative **3** exhibited reasonable activity against bacteria. Overall, derivatives **3** and **4** demonstrated a high ability to inhibit bacterial growth compared to Penicillin G at equivalent concentrations. As a result, these products hold promise as biologically active materials due to the presence of the glucose molecule within their structure, potentially eliminating toxicity and incompatibility.

ACKNOWLEDGMENT

The author thank the advisor Dr. Kareem Alabidi for his continuous guidance and advices during the Ph. D study.

ORCID iDs

Hawraa Sadiq https://orcid.org/0000-0002-1590-0875

REFERENCES

1. Nicolaou KC, Mitchell HJ. Adventures in carbohydrate chemistry: new synthetic technologies, chemical synthesis, molecular design, and chemical biology. *Angew Chem Int Ed Engl.* 2001;40(9): 1576-624. doi:10.1002/1521-3773 (20010518)40
2. Sears P, Wong CH. Carbohydrate mimetics: a new strategy for tackling the problem of carbohydrate-mediated biological recognition. *Angew Chem Int Ed Engl.* 1999;38(16):2300-24. doi:10.1002/(SICI)1521-3773(19990816)38:16<2300::AID-ANIE2300>3.0.CO;2-C
3. Ferrier RJ, Middleton S. The conversion of carbohydrate derivatives into functionalized cyclohexanes and cyclopentanes. *Chem Rev.* 1993;93(8):2779-831. doi:10.1021/cr00023a005
4. Totani K, Takao K, Tadano K. Sugar as a tool for asymmetric synthesis: some effective approaches. *Synlett.* 2004;2004(12):2066-80. doi:10.1055/s-2004-828821
5. Hollingsworth RI, Wang G. Toward a carbohydrate-based chemistry: progress in the development of general-purpose chiral synthons from carbohydrates. *Chem Rev.* 2000;100(12):4267-82. doi:10.1021/cr990123f
6. Hirschmann R, et al. Synthesis of potent cyclic hexapeptide NK-1 antagonists. Use of a minilibrary in transforming a peptidal somatostatin receptor ligand into an NK-1 receptor ligand via a polyvalent peptidomimetic. *J Med Chem.* 1996;39(13):2441-48. doi:10.1021/jm9600439
7. Majik MS, Ghare VM. Green nanoparticles for protection and deprotection reactions in organic synthesis. In: *Nanoparticles in Green Organic Synthesis.* Elsevier; 2023. p.173-93.
8. Govindarajan M. Protecting group migrations in carbohydrate chemistry. *Carbohydr Res.* 2020;497:108151. doi:10.1016/j.carres.2020.108151
9. Varki A. Biological roles of oligosaccharides: all of the theories are correct. *Glycobiology.* 1993;3(2):97-130. doi:10.1093/glycob/3.2.97
10. Wang B, et al. Structural elucidation, modification, and structure-activity relationship of polysaccharides in Chinese herbs: a review. *Front Nutr.* 2022;9:908175. doi:10.3389/fnut.2022.908175
11. Wu J, et al. Site-selective and stereoselective O-alkylation of glycosides by Rh(II)-catalyzed carbenoid insertion. *J Am Chem Soc.* 2019;141(50):19902-10. doi:10.1021/jacs.9b10041
12. Song W, Zheng N. Chiral catalyst-directed site-selective functionalization of hydroxyl groups in carbohydrates. *J Carbohydr Chem.* 2017;36(4-6):143-61. doi:10.1080/07328303.2017.1352634
13. Arunasri K, et al. Effect of simulated microgravity on E. coli K12 MG1655 growth and gene expression. *PLoS One.* 2013;8(3):e57860. doi:10.1371/journal.pone.0057860
14. Jaybhaye A, Deb M. Pathogenesis of Escherichia coli: a clinical findings. *J Pharm Res Int.* 2021;33(60B):3185-91. doi:10.9734/jpri/2021/v33i60B34217
15. Majumdar A, et al. Food degradation and foodborne diseases: a microbial approach. In: *Microbial Contamination and Food Degradation.* Elsevier; 2018. p.109-48.
16. Dhagat S, Jujjavarapu SE. Microbial pathogenesis: mechanism and recent updates on microbial diversity of pathogens. In: *Antimicrobial Resistance: Underlying Mechanisms and Therapeutic Approaches.* Elsevier; 2022. p.71-111.
17. Sabah KJ, Hashim R. Novel mixed-heteroatom macrocycles via templating: a new protocol. *Tetrahedron Lett.* 2013;54(12):1534-37. doi:10.1016/j.tetlet.2013.01.030
18. Bakó P, Töke L. Novel monoaza- and diazacrown ethers incorporating sugar units and their extraction ability towards picrate salts. *J Incl Phenom Mol Recognit Chem.* 1995;23:195-201. doi:10.1007/BF00711536
19. Pham ST, Rapi Z, Bakó P, Petneházy I, Stirling A, Jászay Z. Enantioselective synthesis of substituted α-aminophosphonates catalysed by D-glucose-based crown ethers: pursuit of the origin of stereoselectivity. *New J Chem.* 2017;41(24):14945-53. doi:10.1039/C7NJ02434A
20. Weng-Sieh Z, et al. Synthesis of BxCyNz nanotubules. *Phys Rev B.* 1995;51(16):11229. doi:10.1103/PhysRevB.51.11229
21. Lepage ML, Bodlenner A, Compain P. Stereoselective synthesis of alpha-glycosyl azides by TMSOTf-mediated ring opening of 1,6-anhydro sugars. *Eur J Org Chem.* 2013;2013(10):1963-72. doi:10.1002/ejoc.201201642
22. Hayder T, Aljanaby AAJJ. Antibiotics susceptibility patterns of Citrobacter freundii isolated from patients with urinary tract infection in Al-Najaf Governorate, Iraq. *Int J Res Pharm Sci.* 2019;10(2):1481-88.
23. Vahdati M, Moghadam TT. Synthesis and characterization of selenium nanoparticles-lysozyme nanohybrid system with synergistic antibacterial properties. *Sci Rep.* 2020;10(1):510. doi:10.1038/s41598-019-57350-3
24. Ahmad M, Hawaiz FE. Novel chalcone-based crown ethers: synthesis, characterization, antioxidant activity, biological evaluations, and wastewater remediation. *RSC Adv.* 2024;14(4):2369-79. doi:10.1039/D3RA10175A